Study of barrier height and trap centers of Au/n-$Hg_3In_2Te_6$ Schottky contacts by current-voltage (I-V) characteristics and deep level transient spectroscopy

Yapeng Li, Li Fu,[a] Jie Sun, and Xiaozhen Wang
State Key Laboratory of Solidification Processing, School of Materials Science and Engineering, Northwestern Polytechnical University, Xi'an 710072, China

(Received 31 October 2014; accepted 11 February 2015; published online 25 February 2015)

The temperature-dependent electrical characteristics of the Au/n-$Hg_3In_2Te_6$ Schottky contact have been studied at the temperature range of 140 K–315 K. Based on the thermionic emission theory, the ideality factor and Schottky barrier height were calculated to decrease and increase from 3.18 to 1.88 and 0.39 eV to 0.5 eV, respectively, when the temperature rose from 140 K to 315 K. This behavior was interpreted by the lateral inhomogeneities of Schottky barrier height at the interface of Au/n-$Hg_3In_2Te_6$ contact, which was shown by the plot of zero-bias barrier heights Φ_{bo} versus $q/2kT$. Meanwhile, it was found that the Schottky barrier height with a Gaussian distribution was 0.67 eV and the standard deviation σ_0 was about 0.092 eV, indicating that the uneven distribution of barrier height at the interface region. In addition, the mean value of $\bar{\Phi}_{b0}$ and modified Richardson constant was determined to be 0.723 eV and 62.8 A/cm^2K^2 from the slope and intercept of the $\ln(I_o/T^2) - (q\sigma_0^2/2k^2T^2)$ versus q/kT plot, respectively. Finally, two electron trap centers were observed at the interface of Au/n-$Hg_3In_2Te_6$ Schottky contact by means of deep level transient spectroscopy. © *2015 AIP Publishing LLC*. [http://dx.doi.org/10.1063/1.4913450]

I. INTRODUCTION

As a new photoelectronic material in the near-infrared wavelengths, n-type $Hg_3In_2Te_6$ (short for MIT) single crystals with zinc-blende structure has a number of special properties such as electrical inactivity of the dopants, low defect migration energy, suitable direct band-gap of 0.74 eV at room temperature, high external quantum efficiency, and electrical stability to a very high doze of gamma or neutron radiation.[1–4] Previous research works on MIT crystals are mainly concerned with its electrical properties, optical properties, and crystal or phase structures.[5–8] For MIT photodetectors, it is essential to prepare an electrode film on the surface of MIT to allow carriers to pass through the interface. Various electrode materials such as Au, Ni, and ITO have been selected for the fabrication of Schottky devices up to now.[9–12] However, the distribution of Schottky barrier height (SBH) as well as the deep level defects of Au/MIT Schottky contact are still unclear. Therefore, to deeply understand the formation mechanism of Schottky contact and the deep level defects at the interface between the electrode and MIT substrate, it is essential to study the electrical characteristics of Au/n-MIT Schottky contact under the wide range of temperature.

The near-infrared photodetector device made by MIT is based on the Schottky diode due to its high sensitivity and low leaking current under a certain bias. Typical Schottky contact prepared by different types of materials with a metal-semiconductor (MS) or metal-interlayer-semiconductor (MIS) structure has been intensively investigated due to their wide range of applications in semiconductor devices.[13,14] In particular, the barrier height and ideality factor of the Schottky contact are significant parameters to describe the performance of semiconductor devices.[15] Generally, through the analysis of *I–V* characteristics at room temperature, the detailed information about electrical properties of devices such as current transport mechanism and the formation nature of the barrier height at MS interface cannot be obtained.[16] For the current transport mechanism of a Schottky contact devices, there are many factors which may affect the performance of the devices such as the surface treatment, the interface density of states, contact resistance, temperature, and applied bias voltage.[17] As it is difficult to investigate the carrier transport mechanism under room temperature, it is essential to place the Schottky Barrier Detectors (SBDs) under different temperatures and collect the *I–V* characteristics at the same time.[18–20] In addition, the *I-V-T* characteristics of SBDs based on Thermionic Emission (TE) theory usually reveal an abnormal increase of the Schottky barrier height and a decrease of the ideality factor as well as with the increasing of temperatures.[16,21–24] This is mainly ascribed to the lateral inhomogeneities distribution of Schottky barrier height. At present, a Gaussian distribution of the barrier height for Schottky contact is normally assumed to describe the inhomogeneities.[22,23]

According to the previous research works, there is almost no study on the electrical characteristics of MIT detector with the variation of temperatures. As mentioned above, it is quite important to know the detailed information on the formation and distribution of Schottky barrier under various temperatures as they will greatly affect the performance of devices. In this paper, the *I–V* measurements of Au/n-MIT Schottky contact have been carried out at the different

[a]Author to whom correspondence should be addressed. Electronic mail: fuli@nwpu.edu.cn

temperatures ranging from 140 K to 315 K. Meanwhile, the temperature dependence of barrier height of Au/n-MIT Schottky contact was analyzed by Thermionic emission model, and the Gaussian distribution of barrier heights was calculated at the same time. Moreover, deep level transient spectroscopy (DLTS) has been applied to measure the activation energies of deep levels of Au/n-MIT Schottky contact at different frequencies. Our findings in this paper can be useful to the preparation of semiconductor devices based on Schottky diode.

II. EXPERIMENTAL

MIT single crystal ingots grown by modified vertical Bridgman method were cut into wafers with the size of 5 mm × 5 mm × 1 mm and followed by mechanical polishing. The carrier concentration of MIT wafer was measured to be around $10^{12}\,cm^{-3}$ by means of Hall measurements. After the testing, the wafer was chemical etched by C_3H_7NO:Br_2 (98:2) solution for 30 s to remove the surface damage layer induced by mechanical polishing. After cleaned with acetone, ethanol, and deionized water accordingly, the wafer was dried by nitrogen gas and ready for film deposition. Au and Cu films were prepared by thermal evaporation at the front and back surface of MIT by HHV Auto 306 model vacuum thermal evaporation equipment with the evaporation rate of 0.01 nm/s. Then, by means of the annealing process under N_2 atmosphere at 150 °C an excellent Ohmic contact can be obtained with the contact resistivity of $8.28 \times 10^{-2}\Omega\cdot cm^2$. The elements distribution at the interface of Au/n-MIT Schottky contact was analyzed by SUPRA 55 Field Emission Scanning Electron Microscope (SEM) with an accelerating voltage of 15 kV. *I–V* measurements were performed on DLTS-1000 system at the temperature range of 140–315 K. Furthermore, the deep levels of Au/n-MIT Schottky contact were also tested.

III. RESULTS AND DISCUSSION

Fig. 1 illustrates the *I–V* characteristics of the Au/n-MIT Schottky contact as a function of forward voltage at the temperature range of 140 K–315 K. It is found that the rectifier rate of Au/n-MIT Schottky contact is a little bit lower under each temperature. The reason of low rectifier rate for Au/$Hg_3In_2Te_6$ contact is non-uniformity of surface treatment on $Hg_3In_2Te_6$ wafer, including mechanical polishing, chemical etching, and passivation. This may lead to the interface defect that affecting the electrical properties of Au/n-MIT Schottky contact.[25,26] Meanwhile, it is also found that the leak current increases when the temperature changes from 140 K to 315 K. In this case, the *I–V* characteristics of Au/n-MIT Schottky contact can be analyzed by means of TE model. For bias voltage of $V > 3KT/q$, the relationship between current I and bias V can be defined as follows:[27,28]

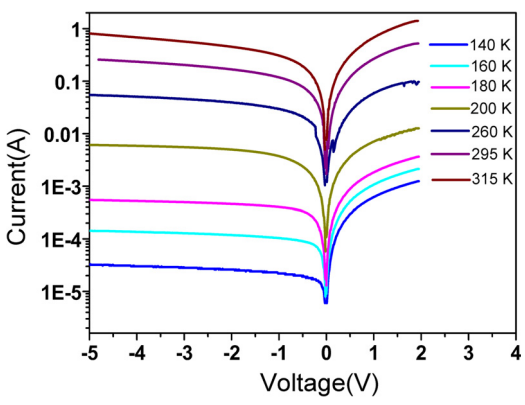

FIG. 1. The *I-V* characteristics of Au/n-MIT Schottky contact under different temperatures.

$$I = I_0 \exp\left(\frac{q(V)}{nkT}\right)\left\{1 - \exp\left(-\frac{q(V)}{kT}\right)\right\}, \tag{1}$$

where k is the Boltzmann constant, n is the ideality factor, T is the absolute temperature, q is the electron charge, and V is the applied voltage. The saturation current I_0 is given by

$$I_0 = AA^*T^2 \exp\left(-\frac{q\Phi_{bo}}{kT}\right) \tag{2}$$

and

$$A^* = \frac{qm_n^*k_0^2}{2\pi^2h^3}, \tag{3}$$

where A is the contact area which is determined to be about $2 \times 2\,mm^2$ and Φ_{bo} is the barrier height under zero-bias. A^* is the effective Richardson constant, q is the electronic charge, and m_n^* is the electron effective mass. The value of m_n^* is determined to be about $0.47m_0$ for MIT according to previous works.[5] From Eq. (3), A^* can be calculated to be $56.505\,A/cm^2K^2$. The values of Schottky barrier height and ideality factor of Au/n-MIT Schottky contact can be determined from the y intercepts and slopes of the forward bias ln$I$ versus V plot at each temperature, respectively. The barrier height can be obtained by rewriting Eq. (2), as shown in Eq. (4). Meanwhile, the ideality factor is determined from the slope of the linear region in the plot of natural log of forward current versus forward bias voltage, which is given in Eq. (5). Here, the linear part of voltage is in the range of 0.1–0.6 V

$$\Phi_{b0} = \frac{kT}{q}\ln\left(\frac{AA^*T^2}{I_0}\right), \tag{4}$$

$$n = \frac{q}{kT}\left[\frac{dV}{d(\ln I)}\right]. \tag{5}$$

According to Eqs. (4) and (5), the values of Schottky barrier height Φ_{b0} and ideality factor n can be obtained in Fig. 2. It is found that the experimental values of Φ_{b0} and n for Au/n-MIT Schottky contact change from 0.3 eV and 3.18 to 0.5 eV and 1.88 when the temperature varies from 140 K to 315 K. This phenomenon is mainly attributed to the transform of current transport mechanisms which obviously deviated from ideal TE model. Actually, there is no widely accepted view for the deviations in non-ideal temperature dependence of the ideality factor and barrier height. One kind of saying is that such deviations may be due to the spatially inhomogeneous of Schottky barrier height as well as the

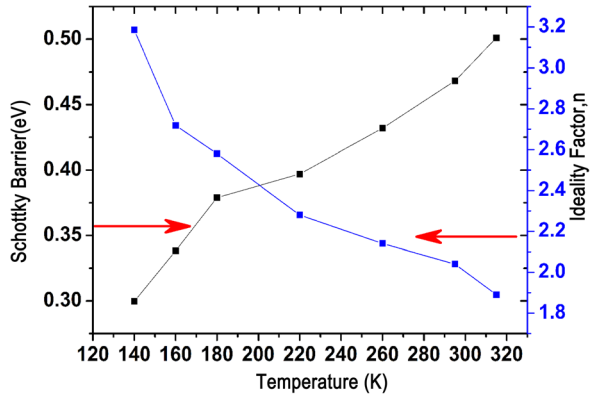

FIG. 2. The variations of the barrier height and ideality factor as functions of temperature.

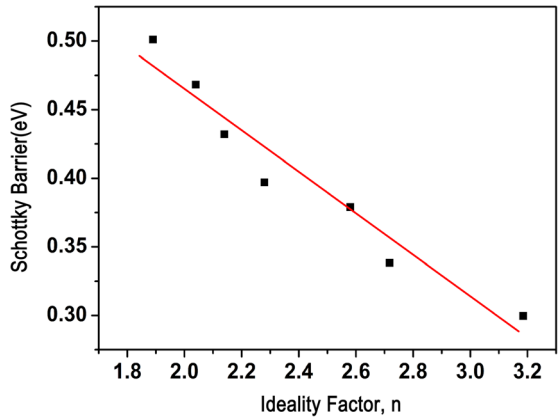

FIG. 4. Schottky barrier height versus ideality factor n.

potential fluctuations at the interface.[30,31] Under this conditions, the inhomogeneous of Schottky barrier height can only be explained by using the Gaussian distribution of the barrier heights. On the other hand, it is well known that the carriers are difficult to go through the higher barrier height under low temperatures due to lack of energy. However, in our cases, the carrier transport existed at the Au/n-MIT Schottky contact interface at the low temperatures as the saturation current at 140 K remains 5.07×10^{-5} A, as shown in Fig. 1. This can be attributed to the lower barrier height with a larger ideality factor at the interface.[27,28] This is an evidence to prove that the carrier transport process are not inhomogeneities across the interface.[32–36]

In addition, some researchers believed that the barrier height was influenced by the interface structure and the element distribution at the interface between metal and semiconductor.[37,38] In this case, the interface morphology and element distribution of Au/n-MIT Schottky contact were analyzed by SEM, as shown in Fig. 3. As seen from the figure, the interface of Au/n-MIT contact reveals a quite close status. No inclusions or holes can be found, as shown in Fig. 3(a). The element distribution at the interface region was also obtained by means of energy dispersive X-ray spectroscopy (EDX). It is noticed that the concentration of Te and In gradually decreased from MIT side to Au electrode, while the concentration of Hg and Au almost remain constant. This is the evidence of inhomogeneous diffusion of different elements across the interface. The uneven distribution of elements may contribute to the inhomogeneous barrier height at last.

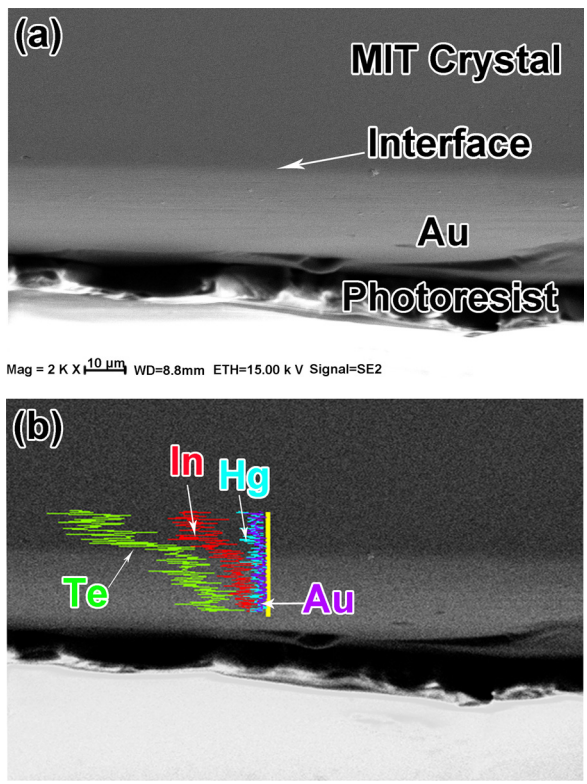

FIG. 3. The interface morphology (a) and element distribution (b) of Au/n-MIT Schottky contact.

The ideality factor is simply a manifestation of the barrier uniformity and will increase for an inhomogeneous barrier. Fig. 4 shows the plot of the zero bias barrier height versus the ideality factor of Au/n-MIT Schottky contact. A linear correlation between the experimental zero-bias barrier height and the ideality factor can be obtained. Furthermore, it is observed that the zero bias barrier height has an inverse proportional to the ideality factors. For the Au/n-MIT Schottky contact, a laterally homogeneous barrier height value can be approximately obtained to be 0.62 eV by the extrapolation of the linear relationship between experimental effective barrier heights and ideality factors to $n = 1$. According to the pinch-off model of Tung, this indicates that the Schottky barrier height is irregularity and can be explained by lateral inhomogeneities of the barrier heights.[39–42] Compared with the homogeneous contact, this inhomogeneity model was usually based on small local patches with lower barrier height at the interface of Au/n-MIT Schottky contact.

Due to the inhomogeneous of the Schottky barrier height, the large variation in ideality factor and zero bias barrier height values cannot be explained using the ideal TE model at low temperature. However, this phenomenon obeys a thermionic emission mechanism with Gaussian distribution of the barrier heights, which is also caused by the presence of the spatially inhomogeneous potential at the MS interface.[29–31] In order to explain this barrier height inhomogeneities, a Gaussian type of distribution functions is

proposed.[18,20,43–45] It is assumed that the distribution of the SBH has a Gaussian distribution and can be expressed as follows:[46]

$$P(\Phi_b) = \frac{1}{\sigma\sqrt{2\pi}}\exp\left[-\frac{(\Phi_b - \Phi_m)^2}{2\sigma^2}\right], \quad (6)$$

where $1/(\sigma\sqrt{2\pi})$ is the normalization constant of the Gaussian BH distribution, σ is the standard deviation, Φ_b is the barrier height, and Φ_m is the mean barrier height. The total current density across a Schottky diode can be expressed as

$$I(V) = \int_{-\infty}^{+\infty} I(\Phi_b, V)P(\Phi_b)d\Phi, \quad (7)$$

where $I(\Phi_b,V)$ is the current at a bias (V) for a barrier height based on the TE model and $P(\Phi_b)$ corresponds to the normalization constant. Therefore, the total current density determined after integrating through the Schottky contact can be given by

$$I(V) = A^*T^2\exp\left[-\frac{q}{kT}\left(\Phi_m - \frac{q\sigma_0^2}{2kT}\right)\right] \times \exp\left(\frac{qV}{n_aKT}\right)\left[1 - \exp\left(-\frac{qV}{kT}\right)\right], \quad (8)$$

where the Gaussian distribution of the apparent barrier height (Φ_m) and variation of the ideality factor (n_a) with temperature are expressed by the following relations:[47]

$$\Phi_a = \Phi_m - \frac{q\sigma_0^2}{2kT} \quad (9)$$

and

$$\left(\frac{1}{n_a} - 1\right) = \rho_2 - \frac{q\rho_3}{2kT}, \quad (10)$$

where ρ_2 and ρ_3 are voltage coefficients, which depends on temperature, with quantifying the voltage deformation of the barrier height distribution.[48]

In order to prove the Gaussian distribution of barrier heights, the experimental relation of Φ_{bo} versus q/2kT and $n^{-1} - 1$ versus q/2kT was drawn from the data of Fig. 1, as shown in Fig. 5. It is found that the temperature-dependent

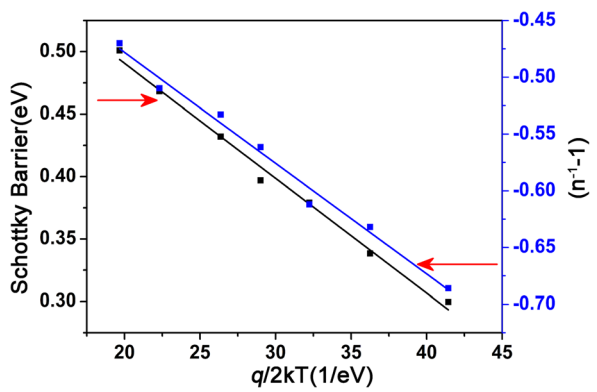

FIG. 5. Schottky barrier height and ($n^{-1} - 1$) versus q/2kT.

characteristics of the Au/n-MIT Schottky contact are consistent with TE model based on the Gaussian distributions of Schottky barrier heights. Fitting of the experimental data in Eqs. (2) and (4) provides Φ_a and n_a, respectively, which obey Eqs. (9) and (10). Thus, the plot of Φ_{bo} versus $q/2k$T should be a straight line which gives Φ_m and σ_0 from the intercept and slope of Fig. 5. The values of ρ_2 and ρ_3 can be determined by the intercept and the slope of the plot $n^{-1} - 1$ versus $q/2kT$ (Fig. 5).

It is assumed that the mean barrier height Φ_b and σ_0 are linearly dependent on voltage and on Gaussian parameters such that $\Phi_b = \Phi_{b0} + \rho_2 V$ and $\sigma_0 = \sigma_{s0} + \rho_3 V$, where ρ_2 and ρ_3 are the voltage coefficients depending on temperature.[28,49] Herein, the temperature dependence of σ_{so} is usually small and can be neglected. From the linear fit, the values of Φ_m and σ_0 can be obtained to be 0.67 eV and 0.092 eV, respectively. When comparing the parameters of Φ_m and σ_0, we find that the standard deviation is 13.7% of the mean barrier height in the temperature range of 140 K–315 K. This indicates that the inhomogeneities of the Schottky barrier height do exist at the interface region. In addition, the obtained values of ρ_2 and ρ_3 are found to be 0.28 eV and 0. 0976 eV, respectively. The linear behavior of this plot also demonstrates that n indeed expresses the voltage deformation of the Gaussian distributions of the Schottky barrier height. Therefore, this inhomogeneity and potential fluctuations dramatically affect the I–V characteristics under low temperatures.

When using Eq. (4) to calculate the Schottky barrier height, the Richardson constant was calculated to be 56.505 A/cm^{2}K^2. However, this constant can change in a wide range of temperature.[50] Therefore, the modified Richardson constant plays an important role during the calculation of the Schottky barrier height, which can be expressed as follows:[51]

$$\ln\left(\frac{I_0}{T^2}\right) - \left(\frac{q^2\sigma_0^2}{2k^2T^2}\right) = \ln(AA^*) - \frac{q\bar{\Phi}_{bo}}{kT}, \quad (11)$$

where $\bar{\Phi}_{b0}$ is the zero-bias mean barrier height, I_0 is the reverse saturation current, and A^* is the modified Richardson constant. In our case, the standard deviation σ_0 is about 0.092 eV by the means of the Gaussian distribution of the barrier heights. Therefore, the $\ln(I_0/T^2) - (q^2\sigma_0^2/2k^2T^2)$ versus $q/2kT$ can be plotted and shown in Fig. 6. The $\bar{\Phi}_{b0}$ and A^* values are determined to be 0.723 eV and 62.8 A/cm^{2}K^2 from the slope and intercept of Fig. 6, respectively. It is found that the modified Richardson value is higher than 56.505 A/cm^{2}K^2. This phenomenon may be due to the spatial inhomogeneous barrier heights and potential fluctuations at the interface. However, such small deviation of the Richardson constant is considered to have less effect on the Schottky barrier height.

It is already known that the carrier transport mechanism may be affected by deep levels at the interface of Schottky contact. Also, the deep levels transient spectroscopy is a capacitance transient thermal scanning method, which is useful to probe a wide variety of deep defects in semiconductor devices.[52] Fig. 7(a) shows the DLTS spectrum for the Au/n-MIT Schottky contact at different lock-in frequencies of 420 Hz, 720

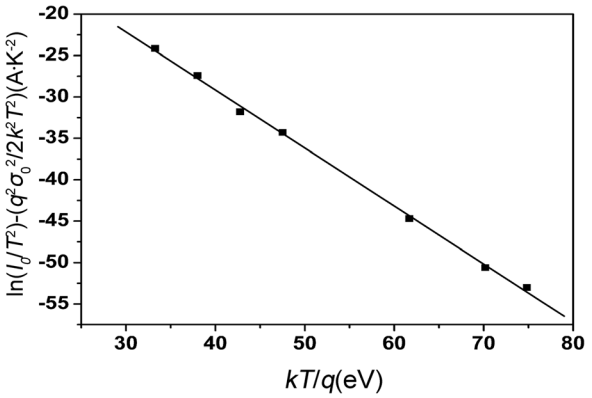

FIG. 6. The plot of modified Richardson, $\ln(I_0/T^2) - (q^2\sigma_0^2/2k^2T^2)$ versus $q/2kT$.

Hz, and 1320 Hz, respectively. The pulse height and width are found to be −1 V and 20 μs, respectively. As shown in Fig. 7, two DLTS peaks can be observed, indicating that two deep trap levels appears for the Au/n-MIT Schottky contact. The densities of the deep trap levels concentration can be determined by peak height in the DLTS spectrum.[53] According the DLTS software analysis, it is found that the deep trap levels concentration are 2.78×10^{16} and $1.13 \times 10^{17}\,\mathrm{cm}^{-3}$ with the activation energies of E_{T1} and E_{T2}, respectively. The values of these deep trap levels concentrations are similar to those in GaAs, CdTe, PbS, and InGaN.[54–57]

When the electron emission dominates the relaxation of the trap states, the electron emission rate (e_n) at an energy level (E_T) can be given by[58]

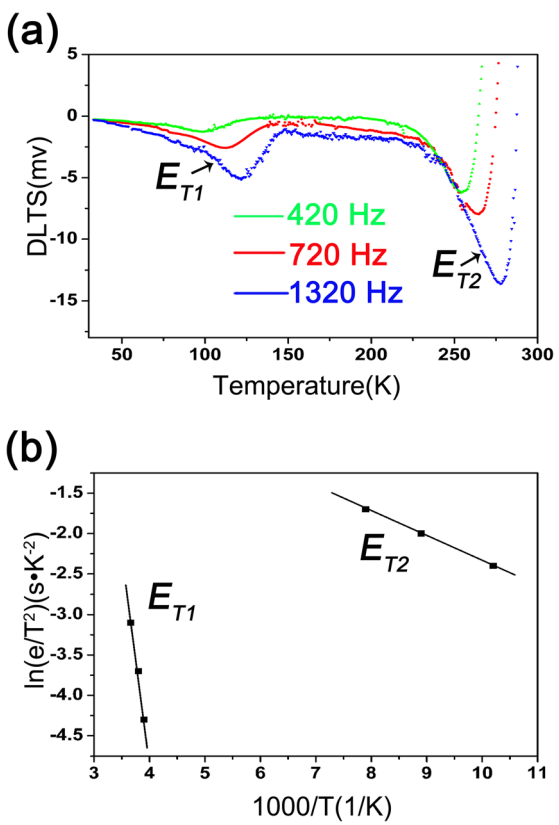

FIG. 7. (a) DLTS spectra for Au/n-MIT Schottky contact. (b) Arrhenius plots of $\ln(e/T^2)$ versus 1000/T for Au/n-MIT Schottky contact.

$$e_n = \sigma_n \gamma T^2 \exp\left(-\frac{E_C - E_T}{\kappa T}\right), \tag{12}$$

where σ_n is the electron capture cross-section, γ is a constant, T is the absolute temperature, k is the Boltzmann constant, and E_C is the conduction band. According to Eq. (12), the electron emission rate exponentially depends on the energy position and temperature. These two factors together with the trap concentration N_t will completely characterizes the corresponding deep level. Therefore, the DLTS peak between the 50 K and 290 K can be attributed to the electron emission from the shallower localized states. The electron-capture process mentioned above in Fig. 7(a) starts to affect the DLTS signal at the temperature of which an infection point occurs on the low-temperature side of the peaks. A peak maximum is reached when the charge decay rate from all the states equals $\ln[(t_0 + t_W)/t_0]/t_W$, where t_0 is the delay time and t_W is the period. Then, the electron emission rate for all states becomes larger than t_0 at high temperature. On the basis of Eq. (12), the following equation can be obtained:

$$\ln\left[\frac{e_n}{T^2}\right] = \ln(\gamma\sigma_n) - \frac{E_C - E_T}{kT}. \tag{13}$$

Thus, the peak temperatures in an Arrhenius-type can be plotted and shown in Fig. 7(b). The linear dependence allows us to extract an activation energy of E_T from the slope and a capture cross-section σ_n from the y-intercept. The calculated activation energies of the two trap centers E_{T1} and E_{T2} are 20 meV and 278 meV, respectively. In addition, at low temperatures, these trap centers may release electrons and participate in the carrier transport process, which lead to inhomogeneities during the current transport process. So far, no additional measurements except for our results have been reported yet on the MIT for deep level defects. For the best of our knowledge, these deep levels probably are caused by vacancy defect of MIT crystal.

IV. CONCLUSIONS

The *I-V* characteristics of Au/n-MIT Schottky contact were investigated under different temperatures. The ideality factor decreased and the Schottky barrier height increased with the increasing of the measurement temperature. The phenomenon was explained by the inhomogeneous barrier height at the interface region. Considering the lateral inhomogeneous distribution of the Schottky barrier height, it is found that the Gaussian distribution best fits situation of Au/n-MIT Schottky contact interface. Meanwhile, the means of Schottky barrier height ($\bar{\Phi}_{bo}$) and Richardson constant (A^*) were determined to be 0.723 eV and 62.8 $\mathrm{A/cm^2K^2}$ from the slope and intercept of the $\ln(I_o/T^2) - (q\sigma_0^2/2k^2T^2)$ versus q/kT plot, respectively. Finally, the DLTS measurement results suggested that the activation energies of the two trap centers E_{T1} and E_{T2} are 20 meV and 278 meV respectively on the interface of Au/n-MIT Schottky contact at the temperature ranging from 50 K to 290 K.

ACKNOWLEDGMENTS

This work was supported by National Natural Science Foundation of China under Contract No. 51172185, the Project of Key areas of innovation team in Shaanxi Province under Contract No. 2014KCT-12, Fund of Ministry of Education for Doctor under Contract No. 20116102110013, the Program of Introducing Talents of Discipline to Universities No. B08040. In addition, the author also thanks Dr. Kukemezey and Dr. Wang in Semilab Semiconductor Physics Laboratory Co. Ltd. very much for their help in the DLTS measurement and data analysis.

[1]G. G. Grushka, Z. M. Grushka, and N. P. Gavaleshko, Ukr. J. Phys. **30**, 304 (1985).
[2]L. P. Galchinetskyi, V. M. Koshkin, and V. M. Kumakov, Soviet Solid St. Phys. **14**, 646 (1972).
[3]V. L. Bakumenko, A. K. Bonakov, and G. G. Grushka, Elektronnaya Technika: Materialy **2**, 75 (1983).
[4]D. M. Spenser and B. Ray, Br. J. Appl. Phys. **1**, 299 (1968).
[5]L. A. Kosyachenko, S. Yu. Paranchich, V. N. Makogonenko, V. M. Sklyarchuk, E. F. Sklyarchuk, and I. I. German, Tech. Phys. **48**, 647 (2003).
[6]O. L. Maslyanchuk, L. A. Kosyachenko, I. I. German, I. M. Rarenko, and V. A. Gnatyuk, Phys. Status Solidi C **6**, 1154 (2009).
[7]J. Sun, L. Fu, H. W. Liu, Y. P. Li, S. P. Ringer, and Z. W. Liu, J. Alloys Compd. **601**, 298 (2014).
[8]J. Sun, L. Fu, H. W. Liu, S. P. Ringer, and Z. W. Liu, J. Alloys Compd. **622**, 206 (2015).
[9]A. I. Malik, G. G. Grushka, and N. R. Tevs, Sov. Phys. Tech. Phys. **35**, 723 (1990).
[10]A. I. Malik and G. G. Grushka, Sov. Phys. Tech. Phys. **35**, 1227 (1990).
[11]L. A. Kosyachenko, I. S. Kabanova, V. M. Sklyarchuk, O. F. Sklyarchuk, and I. M. Rarenko, Phys. Status Solidi A **206**, 351 (2009).
[12]J. Sun, L. Fu, S. P. Ringer, Y. P. Li, and Z. W. Liu, J. Mater. Sci. **49**, 6160 (2014).
[13]X. Lu, X. Xu, N. Q. Wang, Q. Zhang, and M. C. Lin, J. Phys. Chem. B **105**, 10069 (2001).
[14]M. Biber, C. Coşkun, and A. Türüt, Eur. Phys. J. Appl. Phys. **31**, 79 (2005).
[15]G. R. Liang, T. H. Cui, and K. Varahramyan, Microelectron. Eng. **65**, 279 (2003).
[16]S. Shankar Naik and V. Rajagopal Reddy, Superlattices Microstruct. **48**, 330 (2010).
[17]E. Özavcl, S. Demirezen, U. Aydemir, and Ş. Altındal, Sens. Actuators, A **194**, 259 (2013).
[18]J. H. Werner and H. H. Güttler, J. Appl. Phys. **69**, 1522 (1991).
[19]S. Zeyrek, Ş. Altındal, H. Yüzer, and M. M. Bülbül, Appl. Surf. Sci. **252**, 2999 (2006).
[20]S. Zhu, R. L. Van Meirhaeghe, C. Detavernier, F. Cardon, G. P. Ru, X. P. Qu, and B. Z. Li, Solid State Electron. **44**, 663 (2000).
[21]Y. P. Song, R. L. Van Meirhaeghe, W. H. Laflere, and F. Cardon, Solid State Electron. **29**, 633 (1986).
[22]S. Karatas, S. Altindal, A. Turat, and A. Ozmen, Appl. Surf. Sci. **217**, 250 (2003).
[23]A. S. Bhuiyan, A. Martinez, and D. Esteve, Thin Solid Films **161**, 93 (1988).
[24]R. Hackam and P. Horrop, IEEE Trans. Electron Devices **19**, 1231 (1972).
[25]F. Z. Pür and A. Tataroğlu, Phys. Scr. **86**, 035802 (2012).
[26]F. D. Auret, W. E. Meyer, S. Coelho, and M. Hayes, Appl. Phys. Lett. **88**, 242110 (2006).
[27]H. Rhoderick and R. H. Williams, *Metal-Semiconductor Contacts* (Oxford University Press, London, 1988).
[28]V. R. Reddy, D. S. Silpa, V. Janardhanam, H. J. Yun, and C. J. Choi, Electron. Mater. Lett. **11**, 73 (2015).
[29]R. F. Schmitsdorf, T. U. Kampen, and W. Monch, J. Vac. Sci. Technol., B **15**, 1221 (1997).
[30]M. Soylu and B. Abay, Microelectron. Eng. **86**, 88 (2009).
[31]A. A. M. Farag and I. S. Yahia, Synth. Met. **161**, 32 (2011).
[32]E. V. Kalinina, N. I. Kuznetsov, V. A. Dmitriev, K. G. Irvine, and C. H. Carter, J. Electron. Mater. **25**, 831 (1996).
[33]S. Arulkumaran, T. Egawa, H. Ishikawa, M. Umeno, and T. Jimbo, IEEE Trans. Electron Devices **48**, 573 (2001).
[34]Y. Zhou, D. Wang, C. Ahyi, C. C. Tin, J. Williams, M. Park, N. M. Williams, A. Hanser, and E. A. Preble, J. Appl. Phys. **101**, 024506 (2007).
[35]A. R. Arehart, B. Moran, J. S. Speck, U. K. Mishra, S. P. DenBaars, and S. A. Ringel, J. Appl. Phys. **100**, 023709 (2006).
[36]N. Yildirim, K. Ejderha, and A. Turut, J. Appl. Phys. **108**, 114506 (2010).
[37]A. A. Kumar, L. D. Rao, V. R. Reddy, and C. Choi, Curr. Appl. Phys. **13**, 975 (2013).
[38]A. Nawawi, K. J. Tseng, Rusli, G. A. J. Amaratunga, H. Umezawa, and S. Shikata, Diamond Relat. Mater. **35**, 1 (2013).
[39]R. T. Tung, Mater. Sci. Eng., R **35**, 1 (2001).
[40]R. T. Tung, Phys. Rev. B **45**, 13509 (1992).
[41]R. F. Schmitsdorf, T. U. Kampen, and W. Mönch, Surf. Sci. **324**, 249 (1995).
[42]T. Kılıçoğlu, Thin Solid Films **516**, 967 (2008).
[43]S. Chand and J. Kumar, J. Appl. Phys. **80**, 288 (1996).
[44]S. M. Wasim, L. Essaleh, C. Rincon, G. Marin, J. Galibert, and J. Leotin, J. Phys. Chem. Solids **66**, 1887 (2005).
[45]P. Q. Mantas, J. Eur. Ceram. Soc. **19**, 2079 (1999).
[46]A. Gűműş, A. Tűrűt, and N. Yalçin, J. Appl. Phys. **91**, 245 (2002).
[47]S. Fiat, I. Polat, E. Bacaksiz, M. Kompitsas, and G. Cankaya, Curr. Appl. Phys. **13**, 1112 (2013).
[48]S. Fiat and G. Cankaya, Mater. Sci. Semicond. Process. **15**, 461 (2012).
[49]K. V. Madhu, S. R. Kulkarni, M. Ravindra, and R. Damle, Nucl. Instrum. Methods Phys. Res., Sect. B **254**, 98 (2007).
[50]N. Hamdaoui, R. Ajjel, B. Salem, and M. Gendry, Mater. Sci. Semicond. Process. **26**, 431 (2014).
[51]S. Alialy, Ş. Altındal, E. E. Tanrıkulu, and D. E. Yıldız, J. Appl. Phys. **116**, 083709 (2014).
[52]J. H. Evans-Freemana, A. R. Peaker, I. D. Hawkins, and P. Y. Y. Kan, Mater. Sci. Semicond. Process. **3**, 237 (2000).
[53]D. K. Schroder, *Semiconductor Material and Device Characterization* (Wiley, New York, 1998).
[54]R. Boumaraf, N. Sengouga, R. H. Mari, A. Meftah, M. Aziz, D. Jameel, N. A. Saqri, D. Taylor, and M. Henini, Superlattices Microstruct. **65**, 319 (2014).
[55]A. T. Collins and T. C. McGill, J. Vac. Sci. Technol., A **1**, 1633 (1983)
[56]D. Bozyigit, M. Jakob, O. Yarema, and V. Wood, ACS Appl. Mater. Interfaces **5**, 2915 (2013).
[57]E. Gür, Z. Zhang, S. Krishnamoorty, S. Rajan, and S. A. Ringel, Appl. Phys. Lett. **99**, 092109 (2011).
[58]N. M. Johnson, D. J. Bartelink, R. B. Gold, and J. F. Gibbons, J. Appl. Phys. **50**, 4828 (1979).